Environ Earth Sci (2015) 73:5843–5854
DOI 10.1007/s12665-015-4366-y

THEMATIC ISSUE

Perforation spacing optimization for multi-stage hydraulic fracturing in Xujiahe formation: a tight sandstone formation in Sichuan Basin of China

Cong Lu[1] · Jian-Chun Guo[1] · Yu-Xuan Liu[1] · Jian Yin[2] · Yan Deng[1] · Qian-Li Lu[1] · Xing Zhao[1]

Received: 17 September 2014 / Accepted: 29 March 2015 / Published online: 7 April 2015

Abstract Tight reservoir is characterized with low porosity and ultra-low permeability. Horizontal well with multi-stage fracturing is the key technique to maximize stimulated reservoir volume and achieve commercial production. The spacing between perforations has a significant impact on well production. Perforation spacing is currently optimized from the aspects of reservoir simulation. The methods ignore the fact that fracture will generate induced stress field, which may significantly affect the geometry of subsequent fracture. Based on the displacement discontinuity method, this paper established a multi-fracture stress interference model which is able to simulate non-isometric half-length, unequal fracture spacing and arbitrary angle between fracture and wellbore. Data from a tight sandstone reservoir in Sichuan Basin of China are used to analyze the stress field changes and verify the model. The results show that the induced stress creates the maximum compressive stress on both sides of the fracture, and the maximum tensile stress at the fracture tip by stress concentration. The fracture will change the differential horizontal stress ratio in the surrounding area. Position where the differential horizontal stress ratio is lower than 0.3 will be the optimal site to create the complex fractures. Multi-stage fracturing with multiple perforation clusters in one stage is more favorable for complex fracture formation than single perforation cluster in each stage. Data from field verified the proposed perforation optimization method.

Keywords Horizontal well · Fracture spacing optimization · Multi-stage fracturing · Induced stress field · Sichuan Basin of China

List of symbols

a_j	Half-length of element j(m)
D_s^j	Discontinuous in the direction of the s axis (m)
D_n^j	Discontinuous in the direction of the n axis (m)
G	Shear modulus (MPa)
K_h	Differential horizontal stress ratio (–)
L	Half-length of hydraulic fracture (m)
P	Net pressure in fracture (MPa)
β_j	Dip angle (°)
σ_H	Maximum horizontal stresses (MPa)
σ_h	Minimum horizontal stresses (MPa)
$\sigma'_{H(\mathrm{T})}$	Combined stresses in the directions of the maximum horizontal stresses (MPa)
$\sigma'_{h(\mathrm{T})}$	Combined stresses in the directions of the minimum horizontal stresses (MPa)
σ_{lx} (iT)	Induced stress of ith fracture imposes on the Tth fracture in the direction of the x axis (MPa)
σ_{ly} (iT)	Induced stress of ith fracture imposes on the Tth fracture in the direction of the y axis (MPa)
$\Delta\sigma$	Original horizontal stress difference (MPa)
$\Delta\sigma$'	Induced stress difference (MPa)

Introduction

The porosity and permeability of tight sandstone formations are extremely low, and pore structures are generally complex and heterogeneous. Thus, the drainage area per

✉ Jian-Chun Guo
guojianchun@vip.163.com

[1] State Key Laboratory of Oil and Gas Reservoir Geology and Exploitation, Southwest Petroleum University, Chengdu 610500, China

[2] CCDC Drilling and Production Engineering Technology Research Institute, CNPC, Guanghan 618300, China

well is very small. To improve the single well-controlled reserves and deliverability, horizontal drilling and multi-stage hydraulic fracturing have been widely applied in such formations (Waters et al. 2009). The objective of a multi-stage hydraulic fracturing design for horizontal wells is to obtain the highest production (Economides and Tony 2007).

Multi-stage hydraulic fracturing needs to inject large amount of fracturing fluid into the formation. This may cause potential concerns about the environmental problems. Several investigators have focused on this problem, studying the effect of hydraulic fracturing on groundwater in unconventional reservoirs (Kissinger et al. 2013; Lange et al. 2013; Gordalla et al. 2013). Therefore, optimizations are required to achieve the best post-frac production, which reduce the use of fracturing fluid.

Conventional fracturing optimization employs reservoirs simulations to optimize the perforation intervals with predefined fracture morphology. Since, the effect of stress interference between the fractures has not been taken into consideration, which results relatively large spacing and transverse fractures perpendicular to the wellbore. However, due to the extremely low permeability of the matrix in tight sandstone reservoirs, simple major fractures cannot achieve the expected production enhancement. Study has proven that complex fracture network is capable of increasing the matrix conveyance of oil and gas to the fractures, and effectively enhances the production (Holditch 2006). Therefore, it is reasonable to optimize the perforation spacing through the aspect of utilizing fracture interference, which could create a complex stress field and then improve the post-frac response.

It has been well recognized that stress orientation and magnitude in the near wellbore area will change during hydraulic fracturing from field tests (Warpinski and Branagan 1989) and laboratory observations (Wright 1994; Wright and Conant 1995). Initially, the model predicting stress changes was mainly used in refracturing treatment for vertical wells. Sneddon and Elliot (1946) derived an analytical stress model in the vicinity of a crack in an infinite elastic solid. Further, new model was established to describe stress distribution around a penny-shaped crack (Sneddon 1946). According to elastic mechanics and fluid–solid coupling theories, Liu et al. (2004) built an induced stress model for refractured gas wells and developed programs for quantitative analysis of the stress field before refracturing. Deng (2005) developed an induced stress model based on elastic mechanics, and derived the analytical solutions for stress fields induced by fracturing with the aid of the semi-inverse method. Roussel and Sharma (2012) studied the effect of stress induced by both hydraulic fractures and pore pressure on the initiation and propagation of new fractures in a refracturing treatment in horizontal wells. Zhou et al. (2015) also investigated the stress reorientation in tight gas refracturing through a numerical model with combined XFEM and FVM.

Recently, network fracturing in shales becomes a research hotspot, induced stress during multi-stage fracturing has regained great attention. Soliman et al. (2008) analytically studied the interference of stress change on subsequent fractures during multi-stage fracturing by superposition. Later, by examining the stress change between two fractures during multi-stage fracturing in Barnett shale, they related the difference in principal stresses to the distance between two parallel fractures (Soliman et al. 2010). Cheng (2009) numerically calculated the effect of neighboring fractures on stress fields using a commercial software based on the displacement discontinuity method. Roussel and Sharma (2011) explored the orientation and magnitude of the maximum principal stress around the hydraulic fractures through numerical method. The influences of fracture length and width on stress distribution as well as the reorientation of stresses due to fracturing under different in situ stress differences have been discussed in their publication. Rafiee et al. (2012) studied induced stress field around fractures in zipper and modified zipper fracturing, demonstrating that the stress field around the fractures could be effectively altered, to improve the fracture network complexity and enhance production.

The analytical method is derived under the condition of a single fracture. It is not appropriate for calculating the induced stress considering multiple fractures' interaction. The numerical method is computationally expensive, so its application is limited. Thus, there is a need to develop a method which could consider the effect of multiple fracture interaction and also save calculation time.

The displacement discontinuity method (DDM), a simple and convenient tool in dealing with discontinuity problems in rock engineering, is adopted here. This method established by Crouch (1976) solves the relative displacement on the plane of the crack in rock engineering, which resembles the stress field problem in hydraulic fracturing. Thus, in recent years, DDM has gained widely application in hydraulic fracturing treatment, such as the description of hydraulic fracturing propagation (Marina et al. 2014), time-dependent opening and sliding of natural fractures under fluid pressure (Beugelsdijk et al. 2000), modeling of induced stress field around the hydraulic fracture tip (Zhou and Ghassemi 2009), simulating the fracture aperture changes during the injection and flow back by integrating the finite difference method (Jo and Hurt 2013), and investigating the changes of effective stress and fracture permeability in combination with the nonlinear deformation model (Jalali and Dusseault 2011). However, studies of a stress field after the generation of complex fracture networks in unconventional reservoirs are still rare.

Based on the homogeneous and isotropic 2D fracture plane model, this paper develops a stress interference model for dynamic propagation of multiple fractures with arbitrary dip angles, variant half-lengths and intervals. Afterwards, the model is used to investigate the stress field around the horizontal wellbore under dynamic propagation of multiple fractures that occur either sequentially or synchronously. Fracture spacing laterally along the horizontal wellbore is optimized with the minimum differential horizontal stress ratio required for a complex fracture generation in accordance with the experimental findings of Beugelsdijk et al. (2000). Besides, the effect of fracture parameters on the formation of complex fracture networks is analyzed. Data from Xujiahe formation in Sichuan Province of China are adopted here to provide basic parameters and verify the model.

Perforation optimization model for multi-stage fracturing of horizontal well

Stress conditions for complex fracture network formation

Certain stress criterion should be satisfied to create a complex fracture network in tight formations. The fracture pattern is affected by the horizontal stress difference, as can be represented by the differential horizontal stress ratio (Zhou and Ghassemi 2009).

$$K_h = \frac{\sigma_H - \sigma_h}{\sigma_h} \tag{1}$$

where σ_H and σ_h are the maximum and minimum horizontal stresses, respectively.

When the horizontal stress difference and differential horizontal stress ratio are small, hydraulic fractures not only initiate in multiple directions but bifurcate and divert during propagation, generating complex patterns. As the horizontal stress difference and differential horizontal stress ratio increase, maximum horizontal stress plays a more and more important role in controlling the fracture direction. Thus, the development of multiple fractures is suppressed. Experimental findings of Beugelsdijk et al. (2000) showed that: sufficient fracture networks can form when the differential horizontal stress ratio is between 0 and 0.3. If the differential horizontal stress ratio is 0.3–0.5, high net pressure is needed for the formation of complex fracture networks. Once the differential horizontal stress ratio exceeds 0.5, the threshold, hydraulic fracturing cannot create anymore networks. In other words, the smaller the K_h is, the easier the fracture networks could be generated.

An additional stress field induced by the growth of hydraulic fracture changes the original stress field around the wellbore, as shown in Fig. 1. By superposition, the combined stress field after creating T fractures can be expressed as,

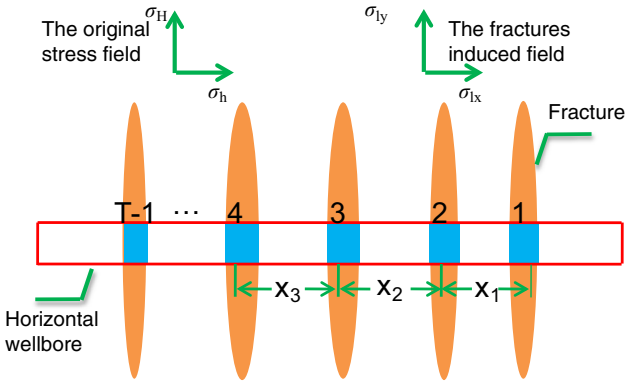

Fig. 1 Sketch of stress distribution around the horizontal wellbore with multi-stage fractures

$$\begin{cases} \sigma'_{\mathrm{H}(T)} = \sigma_{\mathrm{H}} + \sum_{i=1}^{T-1} \sigma_{ly(iT)} \\ \sigma'_{\mathrm{h}(T)} = \sigma_{\mathrm{h}} + \sum_{i=1}^{T-1} \sigma_{lx(iT)} \end{cases} \tag{2}$$

where $\sigma'_{\mathrm{H}(T)}$ and $\sigma'_{\mathrm{h}(T)}$ are, respectively, the combined stresses in the directions of the maximum and minimum horizontal stresses; σ_{lx} (iT) and σ_{ly} (iT) are the induced stress components, which the ith fracture imposes on the Tth fracture.

Equation (1) can be rewritten as,

$$K_{\mathrm{h}} = \frac{\sigma'_{\mathrm{H}(T)} - \sigma'_{\mathrm{h}(T)}}{\sigma'_{\mathrm{h}(T)}} = \frac{\Delta\sigma - \Delta\sigma'}{\sigma'_{\mathrm{h}(T)}} \tag{3}$$

where $\Delta\sigma$ and $\Delta\sigma'$ are, respectively, the original horizontal stress difference and the induced stress difference.

If the induced stress difference is larger than the original horizontal stress difference, the maximum and the minimum horizontal stresses will be inverted and $K_{\mathrm{h}} < 0$. In the inverted area, fractures propagating reorient toward the direction of original minimum horizontal stress direction. For example, generally at the beginning, the horizontal wellbore is aligned in the direction of the minimum horizontal stress without the effect of induced stress, and fractures initiate perpendicular to the wellbore, like fracture 1 in Fig. 2. Due to the additional induced stress, fractures could reorient during propagation to intersect more natural fractures, enhancing the complexity of fracture networks, such as fracture 2 in Fig. 2.

Induced stress model for hydraulic fractures

During the multi-stage fracturing of a horizontal well, net pressure in the hydraulic fracture cause loads on their walls,

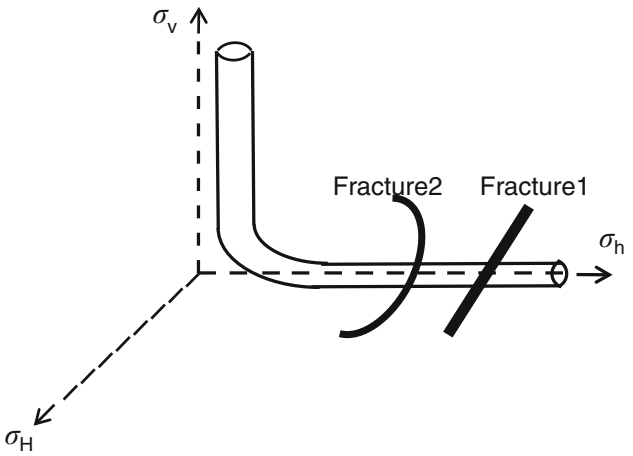

Fig. 2 Schematic diagram of fracture reorientation

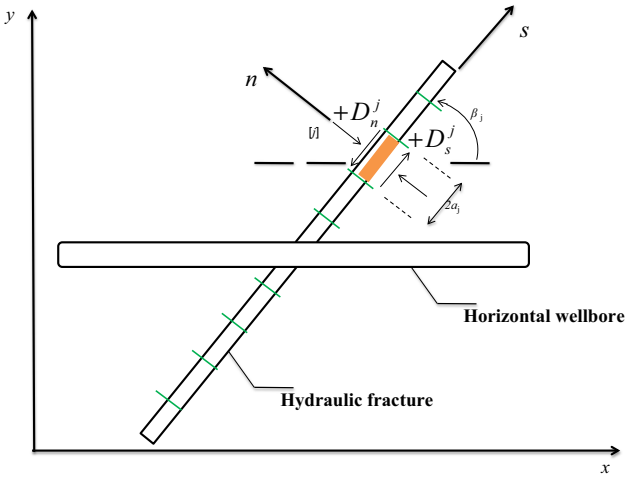

Fig. 3 Sketch of coordinate systems

thus inducing extra stress. For this stress boundary problem, the displacement discontinuity method (DDM) is adopted to derive the induced stress model. The local coordinates (s, n) and global coordinates (x, y) whose x axis is parallel to the wellbore are set up in Fig. 3. For the jth element in total N boundary elements discretized along the hydraulic fracture L, β_j is the dip angle, displacement discontinuous quantities, representing the magnitude of displacements caused by the deformation on the rock surface, are noted by D_s^j and D_n^j. When the fracture planes move toward each other, D_n^j is positive. When the positive side (left side) of the fracture moves to the left with respect to the negative side (right side), D_s^j is positive, as shown in Fig. 3. Compressive stress is positive. Tensile stress is negative.

Stress boundary conditions

The uniform pressure inside the fracture is $\sigma_n = p$, then the boundary conditions of element j are,

$$\sigma_s^j = 0,\ \sigma_n^j = P \quad (j = 1 \cdots N) \tag{4}$$

where P is the net pressure in the fracture.

Mathematical model for fracture-induced stress field

The shear stress and normal stress of element i can be obtained with the displacement discontinuous quantity of element j from the following equations (Cheng 2009),

$$\begin{aligned} \overset{i}{\sigma}_s &= \sum_{j=1}^{N} \overset{i,j}{A}_{ss} \overset{j}{D}_s + \sum_{j=1}^{N} \overset{i,j}{A}_{sn} \overset{j}{D}_n \\ \overset{i}{\sigma}_n &= \sum_{j=1}^{N} \overset{i,j}{A}_{ns} \overset{j}{D}_s + \sum_{j=1}^{N} \overset{i,j}{A}_{nn} \overset{j}{D}_s \end{aligned} \tag{5}$$

where $A_{\mathrm{ss}}^{i,j}$, $A_{\mathrm{sn}}^{i,j}$, $A_{\mathrm{ns}}^{i,j}$, $A_{\mathrm{nn}}^{i,j}$ are influential factors of the stress boundary, whose expressions are

$$\begin{aligned} \overset{i,j}{A}_{ss} &= 2G[-f_{\overline{xy}} \sin 2\gamma - f_{\overline{xx}} \cos 2\gamma - \overline{y}(f_{\overline{xyy}} \sin 2\gamma - f_{\overline{yyy}} \cos 2\gamma] \\ \overset{i,j}{A}_{sn} &= 2G[-\overline{y}(f_{\overline{xyy}} \cos 2\gamma + f_{\overline{yyy}} \sin 2\gamma)] \\ \overset{i,j}{A}_{ns} &= 2G[f_{\overline{xy}} \sin^2 \gamma + f_{\overline{xx}} \sin 2\gamma - \overline{y}(f_{\overline{xyy}} \cos 2\gamma + f_{\overline{yyy}} \sin 2\gamma] \\ \overset{i,j}{A}_{nn} &= 2G[-f_{\overline{xx}} + \overline{y}(f_{\overline{xyy}} \sin 2\gamma - f_{\overline{yyy}} \cos 2\gamma)] \end{aligned} \tag{6}$$

where $\gamma = \beta_i - \beta_j$, $\overline{x} = (x_i - x_j)\cos\beta_j + (y_i - y_j)\sin\beta_j$, $\overline{y} = -(x_i - x_j)\sin\beta_j + (y_i - y_j)\cos\beta_j$, G is the shear modulus; $f(\overline{x}, \overline{y})$ can be expressed as,

$$\begin{aligned} f(\overline{x}, \overline{y}) = -\frac{1}{4\pi(1-\nu)} [\overline{y}(\arctan\frac{\overline{y}}{\overline{x} - a_j} - \arctan\frac{\overline{y}}{\overline{x} + a_j}) \\ - (\overline{x} - a_j) \ln\sqrt{(\overline{x} - a_j)^2 + \overline{y}^2} \\ + (\overline{x} + a_j) \ln\sqrt{(\overline{x} + a_j)^2 + \overline{y}^2}] \end{aligned} \tag{7}$$

where a_j is the half-length of element j, $f_{\overline{xy}}$ and $f_{\overline{xx}}$ are the second-order derivatives of $f(\overline{x}, \overline{y})$, $f_{\overline{xyy}}$ and $f_{\overline{yyy}}$ are the third-order derivatives of $f(\overline{x}, \overline{y})$. Substituting Eqs. (4) into (5) yields the basic equation set for fracture-induced stress field,

$$\begin{aligned} 0 &= \sum_{j=1}^{N} \overset{i,j}{A}_{ss} \overset{j}{D}_s + \sum_{j=1}^{N} \overset{i,j}{A}_{sn} \overset{j}{D}_n \\ p &= \sum_{j=1}^{N} \overset{i,j}{A}_{ns} \overset{j}{D}_s + \sum_{j=1}^{N} \overset{i,j}{A}_{nn} \overset{j}{D}_s \end{aligned} \tag{8}$$

The influential factors in equations can be calculated from Eq. (6). To calculate induced stress at any point, the displacement discontinuous quantity of N elements on the

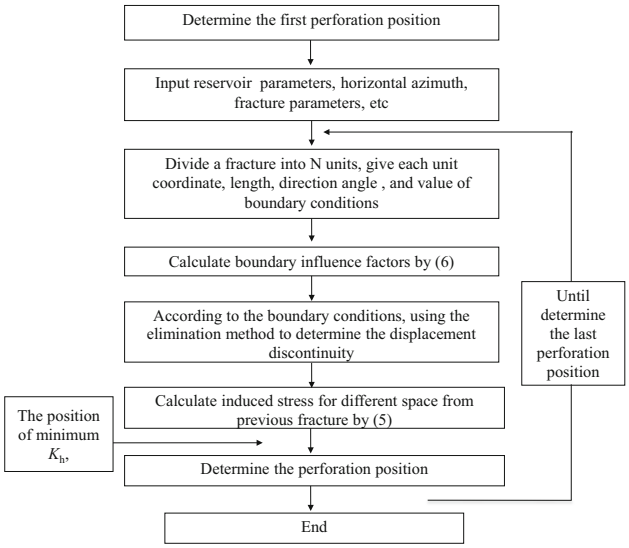

Fig. 4 Flowchart for solving the model

fracture should be calculated by Eq. (8), which consists of $2N$ equations and $2N$ unknowns. With the solved displacement discontinuous quantity of each element, the induced stress at each point can be determined by Eq. (5).

Method for solving the model

As shown in Fig. 4, the facture is evenly divided into N segments. The azimuth, coordinates and boundary conditions are set for each of them. By calculating the boundary influence factors and integrating the boundary element conditions, the displacement discontinuous quantity of each element is determined by the method of iterative elimination. Then, using the coordinates of any location for calculating boundary influence factors of this location, the corresponding induced stress can be computed with the obtained displacement discontinuous quantity. During the optimization of the multi-stage fracturing, the first perforation position is determined from logging results with a good interpretation of gas saturation, porosity and permeability, etc. Then the stress induced by the first fracture at a different distance could be calculated. The perforation of the second interval should be set at the point with the minimum induced stress difference ratio, where complex fracture network tends to form. Afterwards, the perforation position of the third interval can be determined by taking the influence of the first and second fractures into consideration. Similarly, the rest of the perforations can be located successively.

Verification and application of the perforation optimization model

Xujiahe formation is a tight sand formation in Xinchang gas field, China. The target stratum has a deep burial depth up to 5000 m (TVD). The formation is composed of many different types of rock, including glutenite, fine sandstone, siltstone, etc. The rock constituents mainly contain quartz, feldspar and lithoclast. Formation permeability varies from 0.04 millidarcy to 0.78 mD (average 0.13 mD) and porosity from 5 to 12 % (average 7.1 %). It is considered that the formation has a characteristic of low porosity and low permeability. Data from well in this field are used for model verification and application analysis.

The X5H Well is a horizontal well with lateral length 842.3 m, as illustrated in Fig. 5. It is drilled along the direction of the minimum horizontal stress. The target formation is Xujiahe formation with buried depth of 3354 m. The average permeability of the formation is 0.13 mD, average porosity of 7.1 %, so flow capacity of gas to wellbore is bad. To increase the gas production and the recovery, multi-stage fracturing is usually implemented to create fracture networks for improving well production. The parameters used for perforation spacing optimization are: $\sigma_H = 81.4$ MPa, $\sigma_h = 55.8$ MPa, $P = 10$ MPa, fracture half-length $L = 200$ m, formation elastic modulus is 22 GPa, Poisson's ratio is 0.23.

According to logging results of this well, position with good production potential (higher gas saturation, permeability, porosity, etc) could be chose as the first perforation. Depth from 3154.02 to 3154.52 m is determined as the first perforation interval for this well. Then additional stress induced by the first fracture alters the distribution of the maximum and minimum horizontal stresses around the wellbore, as shown in Figs. 6 and 7, respectively. The minimum horizontal stress and horizontal wellbore are in the x direction. The maximum horizontal stress and fracture are perpendicular to the horizontal wellbore. The value of each point, represented by different colors, denotes the stress magnitude. If the magnitude is larger than the original, it means that induced stress is compressive stress and causes an increase in the stress direction. For example, if

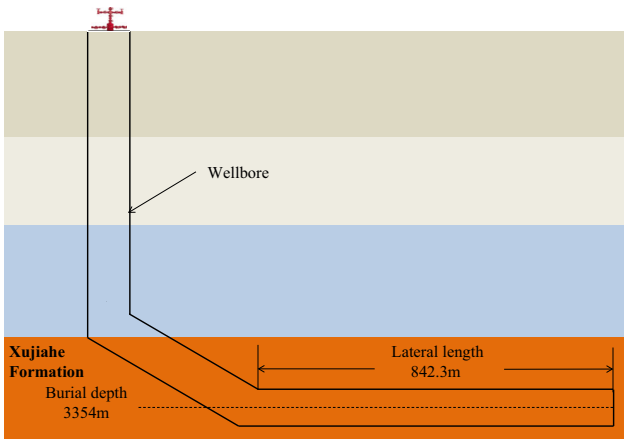

Fig. 5 Schematic diagram of the well configuration

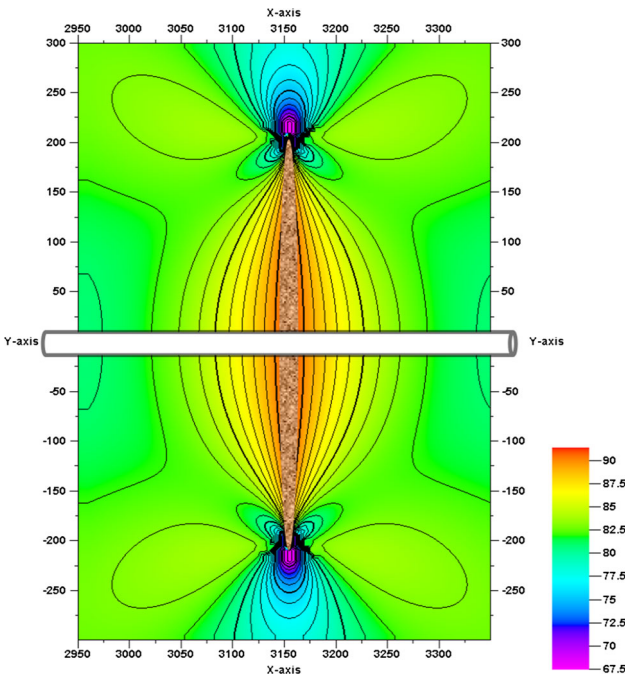

Fig. 6 Maximum horizontal stress distribution around the wellbore after the first fracturing

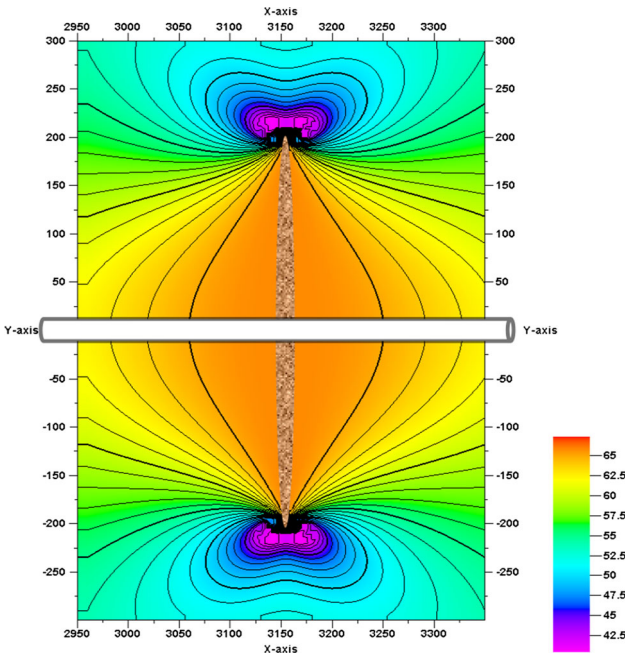

Fig. 7 Minimum horizontal stress distribution around the wellbore after the first fracturing

the stress magnitude at any position in Fig. 7 is larger than 55.8 MPa, it means the induced compressive stress causes an increase in minimum horizontal stress. If the magnitude is less than the original, an induced tensile stress in the stress direction decreases the original compressive stress.

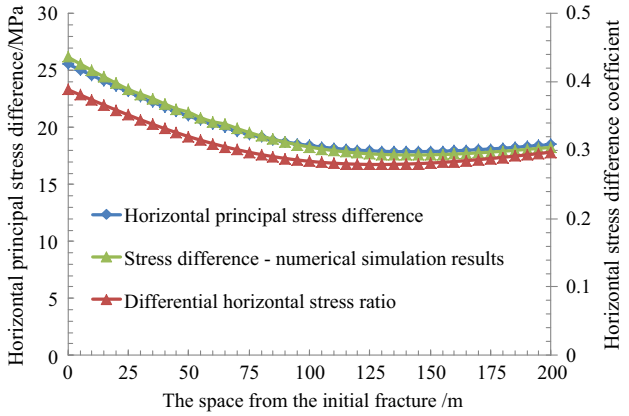

Fig. 8 Horizontal principal stress difference and the differential horizontal stress ratio at different distance from the first fracture

As can be seen from Figs. 6 and 7, the minimum horizontal stress increase from 55.8–65 MPa in the near wellbore region and decrease from 55.8–42.5 MPa near the fracture tip. The trend indicates that the minimum horizontal stress is significantly influenced by the induced stress. The stress change at the fracture tips indicates the local elastic stress concentration, in accordance with existing results (Tao et al. 2009). Although the maximum horizontal stress is also affected by the induced stress, the interference is much smaller than that to the minimum horizontal stress. The maximum horizontal stress only shows obvious increase within 30 m of the fracture, and the purple area denoting induced tensile stress is very restricted.

The horizontal principal stress difference and the differential horizontal stress ratio on the borehole wall that are 0–200 m away from the first fracture are computed, as delineated in Fig. 8.

In Fig. 8, both the horizontal principal stress difference and the differential horizontal stress ratio first decrease and then slightly increase. The minimum values of both parameters emerge at a distance about 130 m away from the first fracture. The minimum horizontal principal stress difference is 17.9, 7.7 MPa lower than the original value. The minimum differential horizontal stress ratio is 0.28, smaller than the critical value of 0.3 for complex fracture generation. Thus, setting the second perforation at 130 m is favorable for the generation of complex fractures during the fracture propagation.

To validate the accuracy of the induced stress model, Abaqus software with finite element framework was utilized for setting up a second model, as shown in Fig. 9. The input parameters used in the simulation is the same as input into DDM model. The simulation result of the stress difference is also illustrated in Fig. 8. The green and blue line overlaps with each other. In another word, both sets of

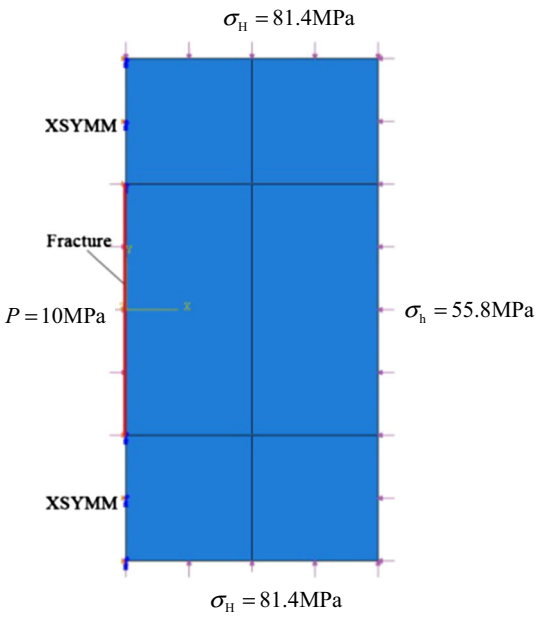

Fig. 9 Finite element model for fracturing-induced stress field

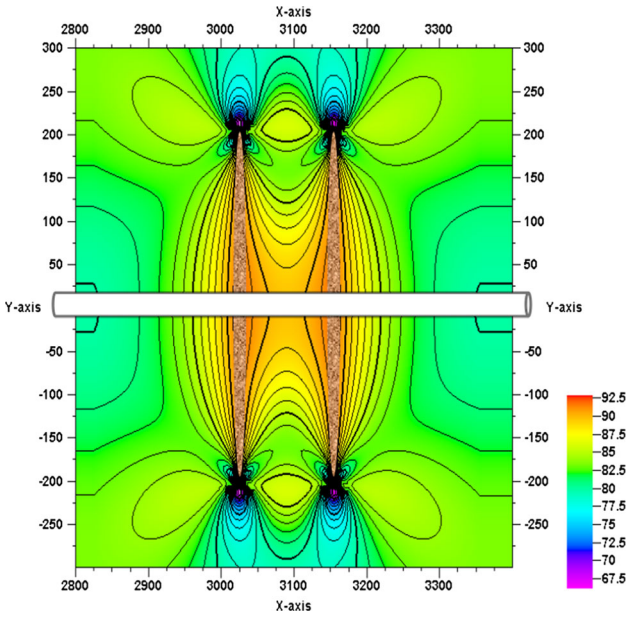

Fig. 10 Maximum horizontal stress distribution around the wellbore after the second fracturing

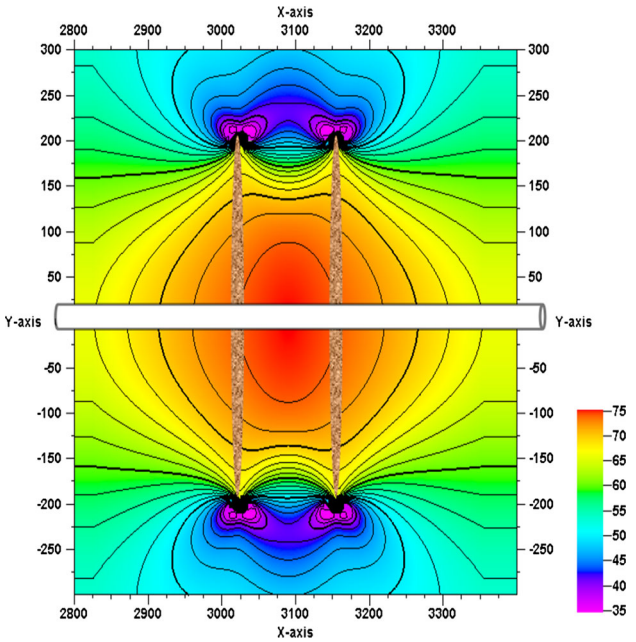

Fig. 11 Minimum horizontal stress distribution around the wellbore after the second fracturing

results are almost the same, verifying the correctness of the DDM model.

Setting the second perforating and fracturing at 3023.02–3023.52 m, the horizontal principal stresses around the horizontal wellbore change, as depicted in Figs. 10 and 11.

As can be seen, the effect of induced stress on the maximum horizontal stress considering two fractures is mainly confined in the vicinity of the fractures, with relatively small magnitude. While for the minimum horizontal stress, the superposition of the interference is substantial, the maximum increment of the minimum horizontal stress reaches 19.3 MPa. Compared with the stress field around a single fracture, multiple fractures interfere with each other, generating a more complex stress field. Table 1 shows that the amplitude of the horizontal stresses increases with the increasing number of fractures.

Similarly, the horizontal stress difference and the differential horizontal stress ratio on the borehole wall that are 0–200 m away from the second fracture were computed, as delineated in Fig. 12. It can be seen that the minimum horizontal stress difference and the minimum differential horizontal stress ratio within 200 m of the first fracture slightly decrease. Based on the spacing of 105 m corresponding to the minimum values of these two parameters, the third perforation is determined at 2918.02–2918.52 m.

By following the above procedures, the differential horizontal stress ratios at different distances from the third to the eighth fracturing are calculated in sequence, as shown in Fig. 13. Consistently, as the fracture spacing increases, all the horizontal stress ratios decrease first and then increase. When the number of fractures exceeds six, the superposed interference inverts the horizontal stresses, the differential horizontal stress ratio $K_h < 0$.

Judging from the minimum differential horizontal stress ratio, the perforation intervals for the third to the ninth fractures are 90, 80, 75, 70, 65 and 65 m, respectively. As the number of perforations increases, the perforation

Table 1 Variation of horizontal stresses after the first and second fracturing

	The maximum horizontal stress (MPa)		The minimum horizontal stress (MPa)	
	The minimum value	The maximum value	The minimum value	The maximum value
Single fracture	67.4	91.4	40.4	65.8
Two fractures	66.1	92.8	34.6	75.1

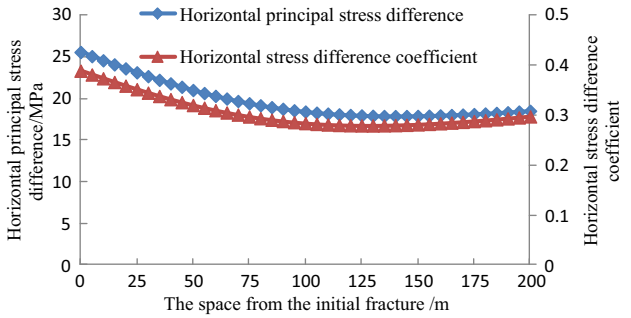

Fig. 12 Horizontal stress difference and the differential horizontal stress ratio at different distance from the second fracture

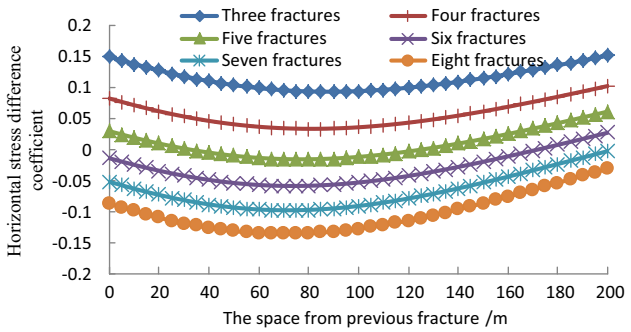

Fig. 13 Differential horizontal stress ratio at different distance from the previous fracture

spacing decreases. But beyond a certain number, the spacing remains constant. Then, perforation positions along the horizontal lateral are determined, as listed in Table 2.

According to the optimized perforation, Xujiahe formation was perforated with a density of 16 shots/m and a phasing of 90°. Nine stages of fracturing were performed by pumping total of 1845.9 m^3 fluid with 265.6 m^3 ceramic proppants of 30–50 meshes. The preflush accounted for 36.7 %, the pumping rate was about 5.0–5.5 m^3, and the proppant concentration of the fracturing fluid was 22.8 %.

In Table 3, the production of this well was much superior in comparison with its adjacent wells, whose completion was designed by numerical simulation. Application of this technique to seven horizontal wells by perforating seven stages with spacing of 89 m on average for each well in the same block yielded an average absolute open flow (AOF) of 12.32 × 10^4 m^3/d, demonstrating the great effectiveness of stimulation.

Results and discussion

Effect of perforation modes on complex fracture network formation

At present, multi-stage fracturing mainly includes two modes: (1) single perforation cluster fracturing, and (2) multiple perforation clusters fracturing. These two methods create different numbers of fractures and associated induced stress at each stage. Simulations were carried out for the well used above with the following specific formation and perforation parameters, as shown in Table 4.

Single perforation cluster

In single perforation cluster fracturing, fractures are primarily dominated by the original horizontal stresses during the propagation. The original differential horizontal stress ratio calculated is 0.46, suggesting the impossibility of generating complex fracture networks.

Additional stress induced by the first fracturing alters the existing horizontal stress field. The difference between the induced stress in the directions of the maximum and minimum horizontal stresses lead to variations in the horizontal stress difference and the differential horizontal stress ratio along the wellbore. Figure 14 depicts the isograms of the differential horizontal stress ratio around the wellbore, showing the stress distribution change due to the induced stress.

As can be seen from Fig. 14, differential horizontal stress ratio in a large area around the wellbore has been reduced to 0.3, which is favorable for complex fracture network generation. Therefore, induced stress caused by opening fracture is beneficial for developing complex fracture networks.

Multiple perforation clusters

Multi-cluster means placing several perforation clusters in each stage in multi-stage fracturing. Mode 2 adopted this peroration mode. Multiple fractures simultaneously initiated and interfered with each from multiple perforations in one stage. Then, the subsequent stage was influenced by these fractures. When three fractures propagated 30 m into the reservoir matrix, the differential horizontal stress ratio around the wellbore was modeled, as shown in Fig. 15.

Table 2 Optimized perforation intervals

Number of fracturing	One	Two	Three	Four	Five	Six	Seven	Eight	Nine
Perforation position (m-m)	3154.02–3154.52	3023.02–3023.52	2918.02–2918.52	2828.02–2828.52	2748.02–2748.52	2673.02–2673.52	2603.02–2603.52	2538.02–2538.52	2473.02–2473.52

During the propagation, three fractures interfered with each other. The deeper the factures propagated, the larger the area the induced stress affects. As the area with differential horizontal stress ratio lower than 0.3 increased, fractures were prone to bifurcate and form complex networks.

Figure 16 gives the distribution of the differential horizontal stress ratio around the wellbore after the fracture propagation. Large reductions in the differential horizontal stress ratio around the fractures will promote the formation of complex fracture networks during the subsequent fracturing treatment.

By comparing these two perforation modes, it is obvious that the mutual interference of fractures in multiple perforation clusters creates the necessary stress conditions for the formation of complex fracture networks. Meanwhile, superposition of induced stresses from previous stages is conducive to fracture network generation in subsequent stages. Thus, multi-stage fracturing with multiple perforation clusters in each stage is more preferable to create complex fracture network.

Effect of fracture parameters on complex fracture network formation

For n fractures in Fig. 17, whether the fracture can form a complex pattern during propagation depend on the differential horizontal stress ratio K_h. From the second fracture, K_h is influenced by the induced stress, which is caused by the previous fractures, therefore, the fracture parameters including length L, net pressure p and fracture space X are all influencing factors.

According to the fracture-induced stress model, net pressure, fracture length and fracture spacing influence the induced stress and the differential horizontal stress ratio. Well X5H was used to analyze the effect of these parameters on the formation of complex fracture networks.

Effect of angle between fracture and wellbore on complex fracture formation

Figure 18 shows the changes in the differential horizontal stress ratio with increasing fracture spacing for different angles between the fracture and the horizontal wellbore.

For different angles, the changes in the differential horizontal stress ratio follow different trends to the fracture spacing increases. When the angle is 30° or 45°, the differential horizontal stress ratio keeps decreasing with increased spacing. While, when the angle is 60° or 90°, the differential horizontal stress ratio first decreases with increasing spacing, and finally tilts up slightly. Results show that with an angle of 90°, the differential horizontal stress ratio is the smallest in all angles, which is favorable for

Table 3 Comparison of fracturing treatments between a well and its adjacent wells

	The length of horizontal section (m)	Number of perforation	The average space (m)	AOF (10^4 m^3/d)
The well	842.3	9	85.0	15.66
Adjacent well I	796.6	5	173.0	5.27
Adjacent well II	912.5	6	157.0	7.43
Adjacent well III	859.6	5	197.0	6.25
Adjacent well IV	789.3	4	213.0	5.43

Table 4 Parameters for computation

The maximum horizontal stress (MPa)	The minimum horizontal stress (MPa)	Horizontal azimuth (°)	Poisson ratio	Young's modulus (MPa)	Mode 1		Mode 2	
					Net pressure of fracture (MPa)	Half-length of fracture (m)	Net pressure of fracture (MPa)	Half-length of fracture (m)
81.4	55.8	90	0.23	22,000	10	100	8	50

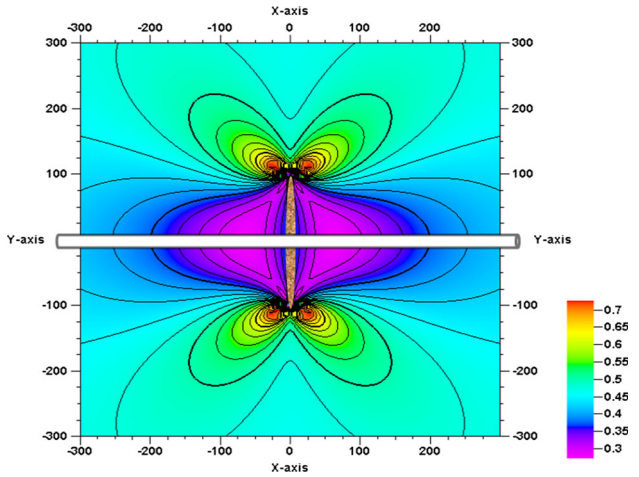

Fig. 14 Change of differential horizontal stress ratio along the horizontal wellbore

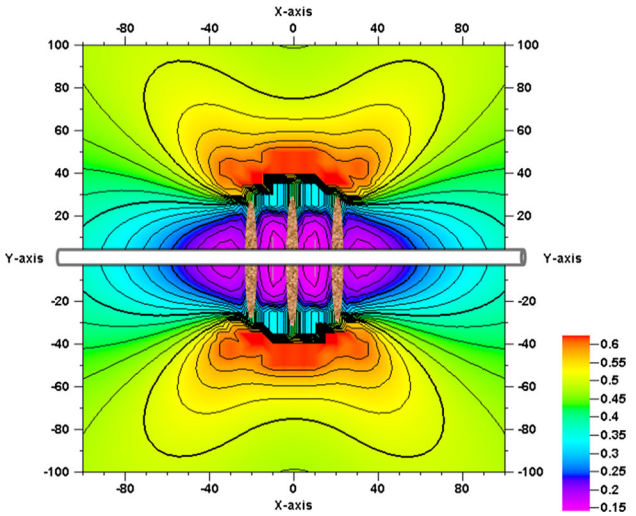

Fig. 15 Change of differential horizontal stress ratio during the fracture propagation

complex fracture generation. Under this condition, the wellbore aligns with the minimum horizontal stress. The effects of net pressure, fracture spacing and length on induced stress are analyzed in the following sections for angles fixed at of 90°.

Effect of net pressure in fracture and fracture spacing on complex fracture network formation

Figure 19 displays the changes in the differential horizontal stress ratio with an increase in fracture spacing under different net pressures.

At a given net pressure, differential horizontal stress ratio first decreases and then increases gently with increasing fracture spacing. That is, there exists a minimum for the differential horizontal stress ratio with respect to the fracture spacing, where complex fracture networks tend to generate. Net pressure does not change the fracture spacing corresponding to the minimum differential horizontal stress ratio. But it does affect the minimum differential horizontal stress ratio. As is obvious, the larger the net pressure, the smaller the differential horizontal stress ratio, the easier the complex fracture networks can form.

Net pressure in a fracture results from reservoir properties and stimulation operating parameters. The former includes elastic modulus, Poisson's ratio and fracture toughness, etc. The latter contains delivery rate, fracturing fluid viscosity, average proppant fluid proportion, etc. The higher the net pressure, the higher the operating pressure needed. Within the nominal pressure in the surface pipeline and pipe string, net pressure should be raised as high as

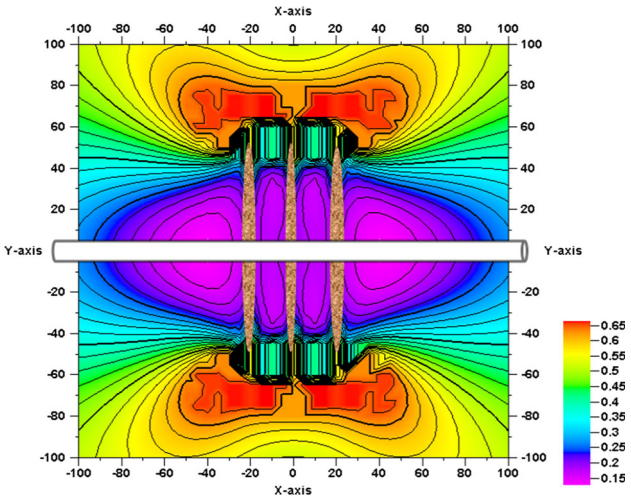

Fig. 16 Change of differential horizontal stress ratio after the fracture propagation

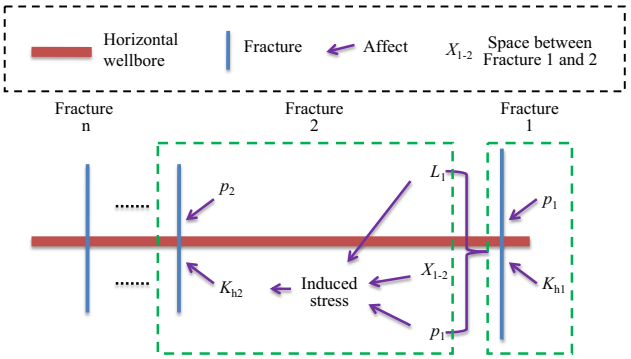

Fig. 17 Effect illustration of fracture parameters on complex fracture network formation

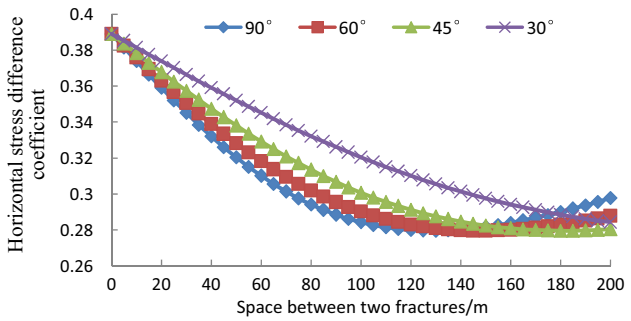

Fig. 18 Effect of angle between fracture and wellbore on the differential horizontal stress ratio

possible to increase the probability of forming complex fracture networks. Fracture spacing and perforation positions should be determined in accordance with the minimum differential horizontal stress ratio for the formation of complex fracture networks.

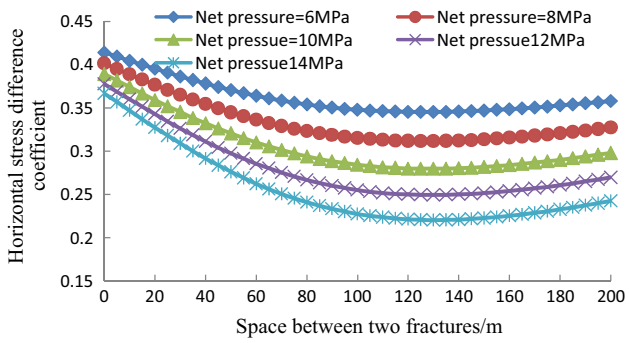

Fig. 19 Effect of net pressure on the differential horizontal stress ratio

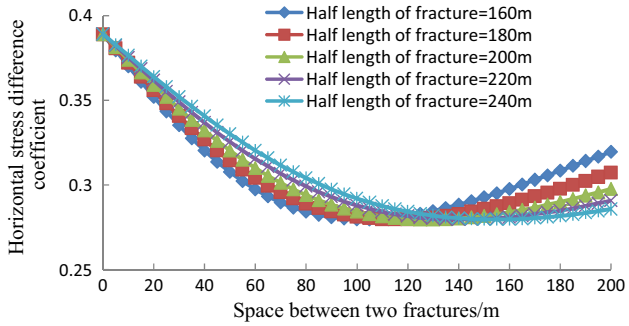

Fig. 20 Effect of fracture half-length on differential horizontal stress ratio

Effect of fracture length on complex fracture network formation

Figure 20 presents the effect of fracture half-length on the differential horizontal stress ratio. Overall, the differential horizontal stress ratio of fractures with different half-lengths first decreases and then increases as the fracture spacing widens. The shorter the fracture, the faster the differential horizontal stress ratio declines with the spacing and the narrower the optimum spacing that corresponds to the minimum differential horizontal stress ratio.

As the fracture half-length increases, the optimum fracture spacing increases. In other words, the interference from the induced stress reaches further into the reservoir with an increasing half-length, resulting in a greater reduction of the differential horizontal stress ratio. This improves the viability of forming complex fracture networks during the subsequent fracturing treatment.

Conclusions

1. The maximum compressive stress is generated at the center of the hydraulic fracture, while the maximum tension occurred at the fracture tips due to the stress

concentration. A 400 m fracture with 10 MPa net pressure is able to change the maximum and minimum horizontal stresses by ±10 MPa.

2. Preformed fractures alter the differential horizontal stress ratio. It is conducive for complex fracture network formations to perforate in areas with a differential horizontal stress ratio lower than 0.3.
3. Data from seven horizontal wells in Sichuan Basin, showed that, with seven stages of fracturing at an interval of 89 m on average for each well, an average AOF of 12.32×10^4 m^3/d was achieved with consideration of induced stress. While average five stages of fracturing with the average interval of 185 m was implemented in an adjacent four wells, which only yielded an AOF of 6.10×10^4 m^3/d. The different AOF between wells demonstrate a prominent effectiveness of the optimization model with consideration of stress interference proposed in this paper.
4. Multi-stage fracturing with multiple perforation clusters in each stage is more favorable for complex fracture formation than single perforation cluster in each stage.
5. Fracture length, net pressure and angle between fracture and wellbore affect the stress induced by fractures. The interference of the induced stress gets larger as the fracture elongates and the net pressure increases, engendering the formation of complex fracture networks during subsequent treatment.

Acknowledgments The authors thank the National Natural Science Foundation of China (51374178) for their financial support.

References

Beugelsdijk LJL, Pater CJD, Sato K (2000) Experimental hydraulic fracture propagation in a multi-fractured medium. In: SPE-59419, SPE Asia Pacific Conference on Integrated Modelling for Asset Management, Yokohama

Crouch SL (1976) Solution of plane elasticity problems by the displacement discontinuity method, Part I. Infinite body solution. Int J Numer Meth Eng 10(2):301–343

Cheng Y (2009) Boundary element analysis of the stress distribution around multiple fractures: implications for the spacing of perforation clusters of hydraulically fractured horizontal wells. In: SPE 125769, SPE Eastern Regional Meeting, West Virginia, USA

Deng Y (2005) Study on mechanical mechanisms of fracture creation in refracturing. Ph.D. Thesis in Southwest Petroleum University, China

Economides MJ, Tony M (2007) Modern fracturing: enhancing natural gas production. ET Publishing Houston, Texas

Gordalla B, Ewers U, Frimmel FH (2013) Hydraulic fracturing—a toxicological threat for groundwater and drinking water? Environ Earth Sci 70(8):3875–3893

Holditch SA (2006) Tight gas sands. J Petrol Technol 58(6):86–93

Jalali RM, Dusseault MB (2011) Hydro-mechanical modeling of fractures with a finite difference-displacement discontinuity method. In: ARMA paper 11-530, 45th US Rock Mechanics/Geomechanics Symposium held in San Francisco, CA

Jo H, Hurt R (2013) Testing and review of various displacement discontinuity elements for LEFM crack problems. In: ICHF paper 2013-021, ISRM International Conference for Effective and Sustainable Hydraulic Fracturing, Brisbane

Kissinger A, Helmig R, Ebigbo A, Class H, Lange T, Sauter M, Heitfeld M, Klünker J, Jahnke W (2013) Hydraulic fracturing in unconventional gas reservoirs—risks in the geological system, Part 2. Environ Earth Sci 70(8):3855–3873

Lange T, Sauter M, Heitfeld M, Schetelig K, Jahnke W, Kissinger A, Helmig R, Ebigbo A, Class H (2013) Hydraulic fracturing in unconventional gas reservoirs—risks in the geological system, Part 1. Environ Earth Sci 70(8):3839–3853

Liu H, Hu Y, Zhao J (2004) Simulation study of induced stress field in refracturing gas well. Chin J Rock Mech Eng 23(23):4022–4027

Marina S, Imo-Imo EK, Derek I, Mohamed P, Yong S (2014) Modelling of hydraulic fracturing process by coupled discrete element and fluid dynamic methods. Environ Earth Sci 72(9):3383–3399

Rafiee M, Soliman MY, Pirayesh E (2012). Hydraulic fracturing design and optimization: a modification to zipper frac. In: SPE 159786, SPE Annual Technical Conference and Exhibition, San Antonio

Roussel NP, Sharma MM (2011) Optimizing fracture spacing and sequencing in horizontal-well fracturing. SPE Prod Oper 26(2):173–184

Roussel N, Sharma MM (2012) Role of stress reorientation in the success of refracture treatments in tight gas sands. SPE Prod Oper 27(4):346–354

Sneddon I (1946) The distribution of stress in the neighbourhood of a crack in an elastic solid. Proc Roy Soc Lond A 187:229–260

Sneddon IN, Elliot HA (1946) The opening of a griffith crack under internal pressure. Quart Appl Math 4(3):262–267

Soliman MY, Loyd EE, David LA (2008) Geomechanics aspects of multiple fracturing of horizontal and vertical wells. SPE Drill Complet 23(3):217–228

Soliman MY, Loyd EE, Jody RA (2010) Fracturing design aimed at enhancing fracture complexity. In: SPE-130043, SPE EUROPEC/EAGE Annual Conference and Exhibition, Barcelona

Tao QC, Economides AE, Ghassemi CA (2009) Modeling variation of stress and permeability in naturally fractured reservoirs using displacement discontinuity method. In: ARMA paper 09-047, 43rd US Rock Mechanics Symposium and 4th US—Canada Rock Mechanics Symposium, Asheville

Warpinski NR, Branagan PT (1989) Altered-stress fracturing. J Petrol Technol 41(9):990–997

Waters G. et al. (2009) Simultaneous hydraulic fracturing of adjacent horizontal wells in the woodford shale. In: SPE 119635, SPE Hydraulic Fracturing Technology Conference, The Woodlands

Wright CA (1994) Reorientation of propped refracture treatments in the lost hills field. In: SPE 27896, SPE Western Regional Meeting, Long Beach

Wright CA, Conant RA (1995) Hydraulic fracture reorientation in primary and secondary recovery from low-permeability reservoirs. In: SPE 30484, SPE Annual Technical Conference and Exhibition, Dallas

Zhou X, Ghassemi A (2009) Three-dimensional poroelastic displacement discontinuity simulation of natural fractures. In: ARMA paper 09-154, 43rd US Rock Mechanics Symposium and 4th US—Canada Rock Mechanics Symposium, Asheville

Zhou L, Gou Y, Hou ZM, Were P (2015) Numerical modeling and investigation of fracture propagation with arbitrary orientation through fluid injection in tight gas reservoirs with combined XFEM and FVM. Environ Earth Sci. doi:10.1007/s12665-015-4051-1